TECHNICAL UNIVERSITY OF CLUJ-NAPOCA

ACTA TECHNICA NAPOCENSIS

Series: Applied Mathematics, Mechanics, and Engineering
Vol. 69, Issue Special III, July, 2026

CALIBRATED ACTIVITY DETECTION IN SENTINEL-1 SAR TIME SERIES

Andrei-Toma STOICA, Simonel-Olimpiu DAVID, Rareș-Cristian BIȘAG

Abstract: *This paper presents a method for facility-scale activity inference from Sentinel-1 SAR time series, emphasizing calibrated change detection under acquisition-geometry variability. Short-window composites are formed around two analysis dates and compared using (i) backscatter change in dB and (ii) standardized anomaly change derived from baseline mean and variance. Detection thresholds are learned from baseline null-pair comparisons via percentile calibration to quantify and control false-alarm behavior. Ascending and descending passes are processed separately to assess geometry-dependent stability. The approach is fully reproducible with open data and yields interpretable AOI-level activity indicators suitable for security monitoring.*

Keywords*: Sentinel-1; synthetic aperture radar; change detection; time-series baselining; false alarm rate; ascending/descending geometry; facility monitoring; global security*

1. INTRODUCTION

Critical infrastructure, including transportation corridors, energy distribution networks, and industrial facilities, is geographically dispersed, continuously evolving, and exposed to both natural hazards and anthropogenic disruption. Maintaining operational integrity therefore requires monitoring approaches that scale across large regions while providing timely, consistent, and auditable information products. Earth observation (EO) is increasingly central to this task because it provides systematic, repeatable measurements that complement in situ inspections and local sensor networks, particularly where access is limited, coverage is uneven, or conditions are dynamic.

Contemporary EO-based monitoring is shifting from isolated image interpretation to time-series detection: the objective is not simply to view a scene, but to detect departures from expected behavior and to quantify their persistence and confidence over time. Within this paradigm, optical multispectral imagery and synthetic aperture radar (SAR) provide complementary capabilities. Optical data offer semantic context and intuitive interpretability, supporting visual corroboration and land-cover discrimination. SAR provides day/night, all-weather continuity and sensitivity to surface structure, moisture, and deformation-related effects, making it especially valuable when optical sensing is degraded by cloud cover, smoke, low illumination, or not possible during the night. However, operational detection from EO time series is challenging because normal background dynamics—seasonality, land-cover phenology, precipitation-driven moisture changes, and viewing geometry effects—can produce strong apparent changes that are not related to the events of interest. Consequently, practical systems must be designed to control false alarms and to communicate uncertainty explicitly.

In security-relevant monitoring, an additional constraint is that the phenomena of interest are often expressed as localized activity rather than clearly labeled damage states.

For example, changes in surface scattering near a facility may indicate construction, ground disturbance, vehicle staging, or other operational activity, but may also be confounded by environmental variability.

This motivates an approach that emphasizes activity inference—a calibrated detection of unusual change relative to a learned baseline - rather than object-level identification or counting. In open-data settings, such as Sentinel-1 GRD SAR, spatial resolution and label scarcity further limit the feasibility of supervised object detection, shifting the methodological focus toward robust, baseline-driven detection and AOI-level indicators suitable for triage.

2. BACKGROUND AND RELATED WORK

Operational infrastructure monitoring requires detecting anomalies against a background of natural variability [7]. While optical sensors provide semantic context, Synthetic Aperture Radar (SAR) offers the necessary all-weather, day/night continuity required for security applications [3,4]. However, SAR change detection is complicated by speckle, moisture variability, and strong geometric dependencies [13].

Traditional approaches often rely on fixed thresholds or supervised deep learning. While deep learning offers high sensitivity, it requires dense labeled datasets that are rarely available for ad-hoc security targets [9,11]. Conversely, standard image differencing is prone to high false alarm rates (FAR) due to environmental noise [7,8].

Recent trends emphasize statistical baselining, where current observations are compared to historical distributions (e.g., z-scores) rather than arbitrary values [7]. This shifts the problem from "object detection" to "anomaly quantification." A critical gap in current operational workflows is the lack of dynamic calibration—specifically, the ability to learn detection thresholds from the location's own history to explicitly control FAR [5,6]. Our method addresses this by combining robust time-series baselining with a "null-pair" calibration strategy, enabling facility-scale activity inference that is reproducible and statistically grounded.

3. PROBLEM FORMULATION AND APPLICATION CONTEXT

Security-relevant facilities and transport nodes are spatially distributed, continuously evolving, and exposed to both natural and anthropogenic risks. Earth observation (EO) supports monitoring at scale through systematic, repeatable measurements. Synthetic aperture radar (SAR) is especially valuable for operational monitoring due to day/night and all-weather imaging, as exemplified by Sentinel-1 [3,4].

Operational use of open SAR archives remains challenging due to speckle, environmental variability (e.g., moisture, vegetation), and acquisition-geometry effects. In particular, ascending and descending passes can induce different backscatter statistics and change responses [4]. Two-date change maps with fixed thresholds therefore risk unquantified false alarms. Meanwhile, supervised object detection generally requires higher spatial resolution and dense labels than open Sentinel-1 GRD provides.

We frame the task as facility-scale activity inference: given an AOI and two analysis dates, determine whether observed SAR change exceeds baseline variability. The method is fully reproducible in Google Earth Engine [14], calibrated using baseline-derived null comparisons, and evaluated separately for ascending and descending acquisition geometries.

The application domain is security monitoring and early-warning triage, where analysts require scalable screening tools that prioritize locations for review. Facility-scale indicators support monitoring of sensitive facilities and logistics nodes by flagging time windows with unusual change relative to historical behavior. This is best interpreted as an alert-for-review mechanism, not object-level counting, at Sentinel-1 GRD resolution.

From a systems perspective, the approach aligns with EO monitoring frameworks emphasizing multi-temporal baselining and explicit false-alarm characterization in time series [7,8].

4. METHODOLOGY AND IMPLEMENTATION

A fixed polygon AOI (Aviabaza Klimovo area) and two analysis dates were defined (t1 = 2021-12-01; t2 = 2022-02-26). Sentinel-1 GRD IW VV scenes were filtered to the AOI and time windows in GEE. Short-window mean composites (±3 days) were generated for t1 and t2, and a baseline composite series was built using a fixed cadence.

Baseline mean and standard deviation were computed to produce standardized anomalies (z-scores). Change scoring used ΔdB and |Δz| between t1 and t2. Thresholds were learned from baseline null pairs by percentile calibration (calibPercentile = 97). Candidate detections were spatially filtered using connected pixel counting (minClusterPixels = 2). The pipeline was executed separately for ASCENDING and DESCENDING passes to quantify geometry dependence.

Sentinel-1 GRD IW VV backscatter was converted to dB:

$$VV_{dB} = 10\, log_{10}(VV + \varepsilon) \quad (1)$$

and temporally averaged in ±3-day windows to reduce variance [4]. Baseline mean μ(x) and standard deviation σ(x) were computed over the baseline period and used to form standardized anomalies:

$$z(x) = \frac{VV(x) - \mu(x))}{\sigma(x) + \delta} \quad (2)$$

Two change scores were computed between the composites:

$$\Delta dB(x) = VV_{t2}(x) - VV_{t1}(x) \quad (3)$$

and

$$|\Delta z(x)| = |z_{t2}(x) - z_{t1}(x)| \quad (4)$$

Thresholds were learned from baseline null pairs: for each consecutive baseline pair, AOI percentiles P97 of ΔdB and |Δz| were computed, and final thresholds were set to the median across null pairs. Candidate pixels satisfy ΔdB > $T_{\Delta dB}$ and |Δz| > $T_{|\Delta z|}$ and are filtered by connected pixel counting (minClusterPixels = 2).

AOI-level indicators include changed area, maximum cluster size, mean |Δz| over candidates, and

$$ActivityIndex = log(1 + area_{ha}) + log(1 + maxClusterPixels) + mean|\Delta z| \quad (5)$$

Empirical FAR is computed on the null series as the fraction of null pairs with ChangedArea_m2 > 0. Pass stratification is used to avoid pooling acquisitions with different viewing geometries [4], improving interpretability and reproducibility [7,8].

5. RESULTS

All results correspond to calibPercentile = 97 and minClusterPixels = 2. The baseline series produced six null pairs per pass (consecutive baseline comparisons).

Table 1 summarizes calibrated thresholds, empirical FAR, and event indicators for ascending and descending acquisitions.

Table 1

Calibrated thresholds and AOI-level activity indicators for Sentinel-1 ascending and descending passes (calibPercentile = 97, minClusterPixels = 2)

Orbit pass	$T_{\Delta dB}$ (dB)	$T_{\|\Delta z\|}$	FAR	Event area (m²)	Event ActivityIndex
ASCENDING	5.289	2.109	0.167	0.000	0.000
DESCENDING	8.210	2.823	0.167	367.159	5.213

ASCENDING calibration yielded T_ΔdB = 5.29 dB and $T_{|\Delta z|}$ = 2.11, while DESCENDING yielded higher thresholds $T_{\Delta dB}$ = 8.21 dB and $T_{|\Delta z|}$ = 2.82. This confirms that baseline tail behavior is geometry dependent for the AOI [4].

Both passes exhibited FAR = 1/6 = 0.167. The ASC baseline alarm occurred on 2021-11-06 (244.8 m²; max cluster 4), while the DESC

baseline alarm occurred on 2021-09-25 (122.4 m²; max cluster 2).

Event detectability diverged: the ASC run produced no candidates (0 m²; ActivityIndex 0), whereas the DESC run produced a non-zero candidate response (367.2 m²; ActivityIndex 5.21). The DESC event exceeds the maximum changed area and ActivityIndex observed across DESC null pairs, suggesting separation from baseline variability under this geometry.

Interpretation of Geometric Dependence. This divergence is physically consistent with the anisotropic scattering nature of man-made structures. In SAR imagery, vertical structures (walls, fences) and vehicles act as strong "double-bounce" scatterers only when aligned orthogonally to the incoming radar pulse [4].

A cluster of vehicles or equipment aligned to reflect strongly in the Descending look-angle may be shadowed or present a low cross-section in the Ascending angle. Â

This result validates the methodological decision to stratify analysis by orbit pass; pooling these geometries would have diluted the signal and obscured the detection.

To support visual interpretation, map products are rendered using fixed radiometric scales derived from the AOI statistics. Mean intensity composites (t_1 and t_2) are visualized in grayscale from **-25 dB (black)** to **0 dB (white)**; this range highlights strong metallic scatterers (bright) against the natural background (darker).

Change maps (dB) utilize a diverging Blue-White-Red color palette clamped at **3 dB**:

- **Blue (≤ Δ -3 dB):** Represents a significant loss in backscatter (e.g., movement of an object away from the pixel).
- **White (~0 dB):** Represents stability or noise within the baseline variance.
- **Red (≥ +3 dB):** Represents a significant increase in backscatter (e.g., arrival of equipment or construction).

Binary detection masks display clusters that satisfy both the calibrated intensity threshold ($T_{\Delta dB}$) and the anomaly threshold ($T_{|z|}$), filtered by a minimum connectivity size of 2 pixels. All maps are oriented North-Up.

5.1 Map products



Fig. 1. ASCENDING VV(t1) mean composite (dB). Intensity is scaled [-25, 0] dB. Bright features correspond to permanent infrastructure and metallic objects.



Fig. 2. ASCENDING VV(t2) mean composite (dB). Intensity is scaled [-25, 0] dB. Bright features correspond to permanent infrastructure and metallic objects.



Fig. 3. ASCENDING Backscatter Change Map ΔdB = VV(t2) − VV(t1) (dB). The blue-white-red palette (±3 dB) reveals just coherent clusters of increased scattering (red), but limited compared to DESCENDING clusters



Fig. 4. ASCENDING candidate mask (binary), calibPercentile = 97, minClusterPixels = 2. No activity clusters exceeded the learned thresholds ($T_{\Delta dB}$=5.29, $T_{|z|}$=2.11).

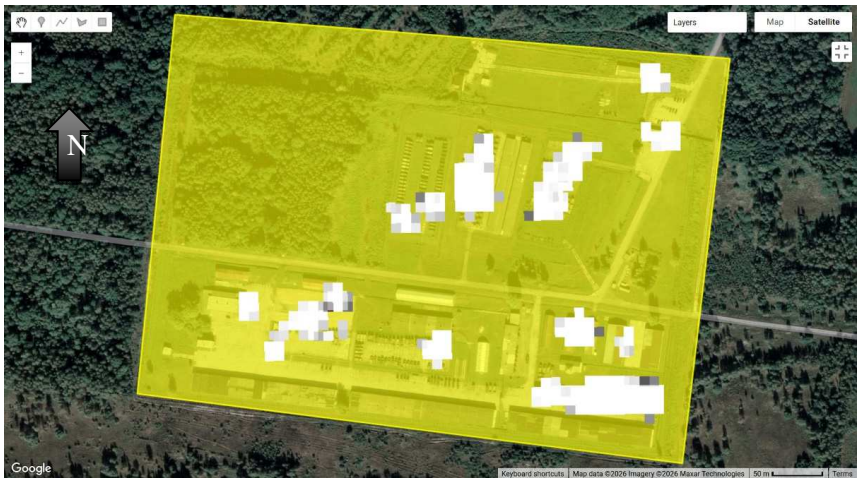


Fig. 5. DESCENDING VV(t1) mean composite (dB). Note the distinct scattering geometry compared to Figures 1-2.

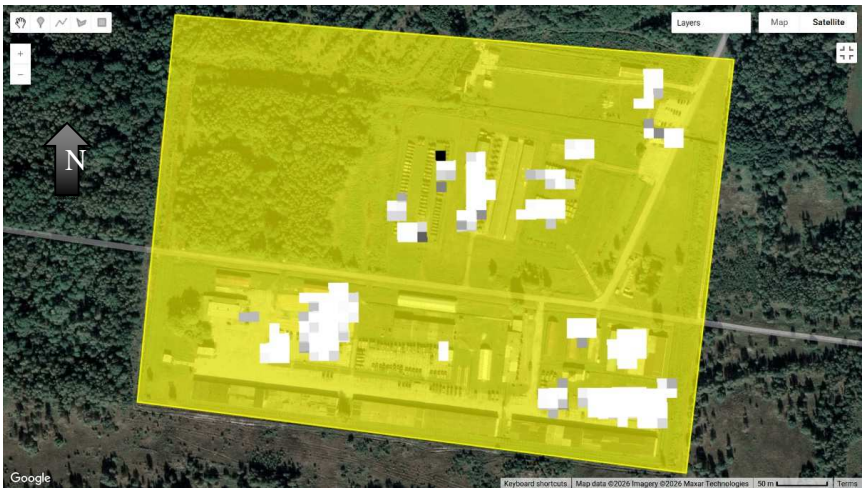


Fig. 6. DESCENDING VV(t2) mean composite (dB). Note the distinct scattering geometry compared to Figures 1-2.

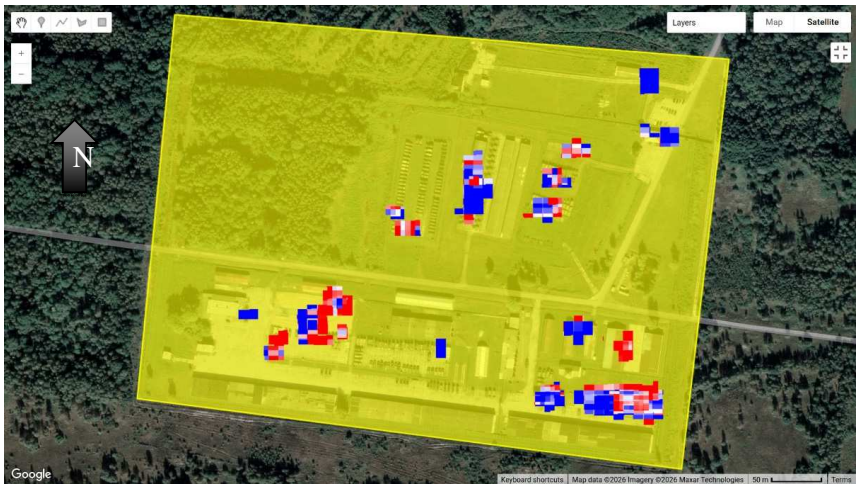


Fig. 7. DESCENDING Backscatter Change Map ΔdB = VV(t2) − VV(t1) (dB). Unlike the stable ASCENDING pass, this geometry reveals distinct clusters of red pixels (increase ≥ +3 dB) and blue pixels (decrease ≤ -3 dB). This spatial mix suggests dynamic operational turnover, such as the simultaneous arrival (red) and departure (blue) of mobile assets.

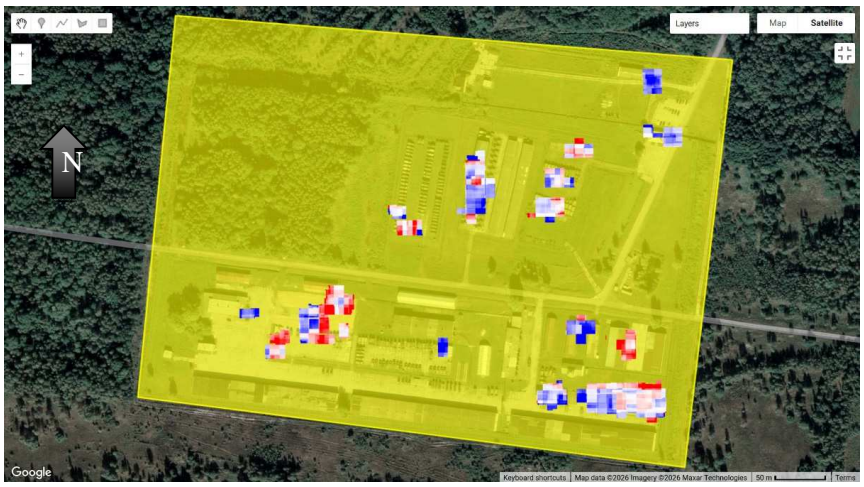


Fig. 8. DESCENDING candidate mask (binary), calibPercentile = 97, minClusterPixels = 2. White pixels highlight the confirmed event cluster (367 m²), which passed the calibrated thresholds ($T_{\Delta dB}$=8.21, $T_{|z|}$=2.82).

6. DISCUSSION AND LIMITATIONS

The proposed method successfully identified localized activity by filtering out background noise using learned thresholds. By calibrating against "null pairs" (periods of known stability), the system provides an empirical estimate of the False Alarm Rate (FAR), offering analysts a confidence metric that simple differencing lacks.

Despite the promising results, two key limitations must be addressed in future work:

- **Temporal Sampling:** The current validation period is relatively short. A longer sampling period covering a full annual cycle is necessary to fully assess the impact of seasonal transitions (e.g., snow melt or heavy vegetation growth) on the baseline variance [7,13].
- **Spatial Resolution:** At Sentinel-1's 10m resolution, the method functions as a "triage" tool. It detects the *presence* of activity but cannot resolve object counts or specific vehicle types. It is best deployed as a cueing mechanism to task higher-resolution optical or SAR sensors [12].

7. CONCLUSIONS

This paper presented a reproducible, GEE-native pipeline for calibrated facility monitoring. Unlike rigid thresholding methods, our approach adapts to the specific noise characteristics of the Area of Interest (AOI) via percentile calibration on baseline null pairs.

The analysis demonstrated that facility-scale activity is highly geometry-dependent; the detection of a significant event in the Descending pass (ActivityIndex 5.21) versus stability in the Ascending pass proves that operational monitoring must treat orbit directions as distinct sensing channels. Future work will focus on extending the baseline window to account for seasonal hysteresis, further improving the robustness of automated security alerts.

8. REFERENCES

[1] European Space Agency (ESA). *Sentinel-2: Observing the Earth (Copernicus). ESA mission overview*. https://www.esa.int/Applications/Observing_the_Earth/Copernicus/Sentinel-2

[2] Copernicus Data Space Ecosystem. *Sentinel-2 Documentation (MSI bands and spatial resolutions)*. https://documentation.dataspace.copernicus.eu/Data/SentinelMissions/Sentinel2.html

[3] Alaska Satellite Facility (ASF). *Sentinel-1 documentation: C-band frequency, revisit characteristics, modes*.

https://webdocs.asf.alaska.edu/Sentinel-1/Sentinel-1-User-Guide.pdf

[4] NASA Earthdata. *Sentinel-1 platform overview and repeat-pass observations*. https://www.earthdata.nasa.gov/data/platforms/space-based-platforms/sentinel-1?

[5] Rosen, P. A., Hensley, S., Peltzer, G., & Simons, M. (2000). *Synthetic Aperture Radar Interferometry*. Proceedings of the IEEE.

[6] Pepe, A., et al. (2017). *A Review of Interferometric Synthetic Aperture RADAR (InSAR) Techniques. Applied Sciences*.

[7] Zhu, Z. (2017). *Change detection using Landsat time series: review of frequencies, preprocessing, algorithms, and applications*.

[8] Fu, Y., et al. (2024). *Remote Sensing Time Series Analysis: A Review of Data, Methods, and Applications*. Science Partner Journal.

[9] Bai, T., et al. (2023). *Deep learning for change detection in remote sensing*.

[10] Saidi, S., et al. (2024). *Deep-Learning for Change Detection Using Multi-Modal Remote Sensing*. Remote Sensing (MDPI).

[11] Peng, D., et al. (2025). *Deep learning change detection techniques for optical remote sensing imagery: a review.*

[12] Copernicus Sentinel Portal. *Sentinel Data Access Overview and Copernicus Data Space Ecosystem positioning*.

[13] Murakami, T. (2025). *Comparative assessment of LandTrendr, CCDC, and BFAST for time-series change detection*. Remote Sensing (MDPI).

[14] Gorelick, N., et al. (2017). *Google Earth Engine: Planetary-scale geospatial analysis for everyone*. Remote Sensing of Environment.

Detecția calibrată a activității în serii temporale SAR Sentinel-1

Rezumat: Această lucrare prezintă o metodă de inferență a activității la scară de obiectiv (facility-scale) din serii temporale SAR Sentinel-1, punând accent pe detecția calibrată a schimbărilor în condițiile variabilității geometriei de achiziție. Se construiesc compozite pe ferestre scurte în jurul a două date de analiză și se compară folosind (i) variația retroîmprăștierii în dB și (ii) schimbarea anomaliilor standardizate, derivată din media și variația unei perioade de referință (baseline). Pragurile de detecție sunt învățate din comparații „null-pair" din perioada de referință, prin calibrare pe percentile, pentru a cuantifica și controla comportamentul de alarmă falsă. Trecerea pe orbită ascendentă și descendentă este procesată separat pentru a evalua stabilitatea dependentă de geometrie. Abordarea este complet reproductibilă folosind date deschise și produce indicatori interpretabili ai activității la nivel de zonă de interes, adecvați pentru monitorizarea de securitate.

Andrei-Toma STOICA, PhD candidate, National University of Science and Technology POLITEHNICA Bucharest, Faculty of Automatic Control and Computers, Computers and Information Technology, andrei_toma.stoica@stud.acs.upb.ro, +40 214 029 100, 313 Splaiul Independentei, Bucharest, Romania.

Simonel-Olimpiu DAVID, MSc Student, Babeș-Bolyai University, Faculty of Mathematics and Computer Science, Distributed Systems in Internet Masters, simonel.david@stud.ubbcluj.ro, +40 264 405 300, 1 Mihail Kogalniceanu Street, Cluj-Napoca, Romania.

Rareș-Cristian BIȘAG, PhD candidate, National University of Science and Technology POLITEHNICA Bucharest, Faculty of Entrepreneurship, Business Engineering and Management, rares.bisag@upb.ro, +40 214 029 100, 313 Splaiul Independentei, Bucharest, Romania.